Journal of Ovonic Research Vol. 12, No. 2, March - April 2016, p. 95 - 102

NEW STUDIES OF PHYSICAL PROPERTIES OF FUNCTIONALIZED SINGLE WALL CARBON NANOTUBES BASED HYBRID PHOTOVOLTAIC CELLS

J. AL-ZANGANAWEE[a,b], S. IFTIMIE[c], T. MUBARAK[b], A. RADU[c], O. BRINCOVEANU[a,c], S. ANTOHE[c,d], M. ENACHESCU[a,d*]
[a]*Center for Surface Science and Nanotechnology (CSSNT), University Politehnica of Bucharest, Romania*
[b]*Physics Department, College of Science, University of Diyala, Iraq*
[c]*University of Bucahrest, Faculty of Physics, MDEO R&D Center, Bucharest, Romania*
[d]*Academy of Romanian Scientists, Bucharest, Romania*

We report the fabrication and characterization of the photovoltaic cells based on functionalized single wall carbon nanotubes (F-SWCNTs) and poly(3-octylthiophene-2,5-diyl) conductive polymer, P3OT. The multilayered photovoltaic structures were prepared by spin-coating. Synthesis of SWCNTs with diameters smaller than 1.6 nm was done using an original recipe and their functionalization by nitric acid was confirmed by thermogravimetric measurements and field emission scanning electron microscopy (FESEM). We performed first experiments of an active layer formed by different percentages of F-SWCNTs (1%, 2% and 4%) mixed with P3OT, finding an optimal one of 2% mixture, as determined for our prepared structures. Performances of fabricated F-SWCNTs:P3OT based photovoltaic cells were compared with P3OT active layer samples in solar simulator conditions (A.M. 1.5) and the enhancement of specific parameters due to F-SWCNTs addition was proved.

(Received February 15, 2016; Accepted April 8, 2016)

Keywords: SWCNTs, functionalization, P3OT, photovoltaic cells

1. Introduction

Tremendous efforts were done during the last twenty years to improve stability and to increase the power conversion efficiency of organic and inorganic photovoltaic cells. A special attention was paid to conductive polymers due to their remarkable physical and chemical properties and cheap deposition techniques [1-4] and to single wall carbon nanotubes (SWCNTs) due to their high values of the electrical conductivity [5, 6]. Important results were reported already for regioregular polymer:fullerene derivative mixture or regioregular polymer/inorganic thin films as active layers or buffer layers, in the architecture of photovoltaic cells [7-9]. Poly(3-octylthiophene-2,5-diyl), P3OT, a π-conjugated polymer, proved to have an early crystalline arrangement, as thin film, with well-define crystalline regions embedded in an amorphous matrix [5, 10-15]. This early crystalline structure facilitates the charge carriers' transport. On the other hand, a good dispersion of single wall carbon nanotubes (SWCNTs) used in different mixtures with organic semiconductors is the key factor to increase their electrical conductivity in order to increase the photovoltaic performances of some hybrid photovoltaic cells, facilitating the charge carriers' transport paths [16-20]. Usually, bundles of SWCNTs due to Van der Waals interactions can be observed [16] limiting the flow of electric current when forward or reverse bias voltage is applied and the chemical interactions. Functionalization of SWCNTs by nitric acid seems to offer a simple way to increase their electrical performances and to reduce bundles number but also can induce changes of hybridization from sp^2 to sp^3 [5, 16, 21, 22].

* Corresponding author: marius.enachescu@upb.ro

In this paper we report the synthesis of SWCNTs using an original recipe and their functionalization by nitric acid. Spectroscopic analyses, thermogravimetric measurements and morphological investigations were done in order to prove that functionalized-SWCNTs (F-SWCNTs) can be used as photoactive layer of photovoltaic cells. Different weight ratios of F-SWCNTs were mixed with P3OT to form bulk-heterojunction photovoltaic structures and after their characterization an optimal percentage of 2% of F-SWCNTs, in F-SWCNTs:P3OT blend was determined. Moreover, for all F-SWCNTs:P3OT active layer samples an increase of external quantum efficiency was observed, as comparing with that of photovoltaic cells based on the single active layer of P3OT. The use of F-SWCNTs as constitutive of active layer hybrid photovoltaic cells is, as far as we know, totally new.

2. Experimental procedures

2.1. Single wall carbon nanotubes

Single wall carbon nanotubes were fabricated by laser ablation using a 248 nm KrF excimer laser with energy of 650 mJ and frequency of 30 Hz. The targets were prepared following an original recipe, mixing graphite cement (GC 8010-B, Metal Forming Lubricants Co.) with metal micro-sized powder of nickel and cobalt (Ni, Co, Sigma Aldrich Co.). The percent ratio used was 98.8% C: 0.6% Ni: 0.6% Co. To improve the mechanical stability, the resulting mixture was cured four hours at 130°C followed by a four hours thermal treatment at 800°C in nitrogen atmosphere. Working parameters of the ablation procedure such as pressure, temperature and time were 500 Torr, 1100°C and 1 hour, respectively.

The fabricated single wall carbon nanotubes (SWCNTs) were functionalized using nitric acid solution 5M, as described by:

$$\text{Pristine SWCNTs} \xrightarrow[50\,^{\circ}\text{C}\ \ 5\ \text{h ultrasonic water bath}]{5\ \text{M}\ HNO_3} \text{COOH Functionalized SWCNTs}$$

2.2. Photovoltaic cells

Onto optical glass substrates covered with an indium tin oxide thin film (ITO, 8 – 12 Ω/cm^2), as anode, the active layer of the photovoltaic cells as a mixture of a regioregular polymer, poly(3-octylthiophene-2,5-diyl) P3OT, and functionalized single wall carbon nanotubes (F-SWCNTs) was deposited by spin-coating. The used F-SWCNTs weight percentages were 1%, 2% and 4%. To improve the homogeneity, an ultrasonic bath was used to blend the solutions for 1 hour at 40°C. A buffer layer of poly(3,4-ethylenedioxythiophene)-poly(stryrenesulfonate) (PEDOT:PSS) was deposited between the ITO thin film and the active layer by spin-coating, to increase the hole's collection to anode. To complete the photovoltaic cells architecture, aluminum cathode (Al) was deposited by thermal evaporation (TE) forming a glass/ITO/PEDOT:PSS/F-SWCNTs:P3OT/Al solar cell. Their photovoltaic performances were compared with those obtained for glass/ITO/PEDOT:PSS/P3OT/Al samples. The architecture of fabricated photovoltaic cells is presented in figure 1 together with the band offset diagram of the constitutive materials.

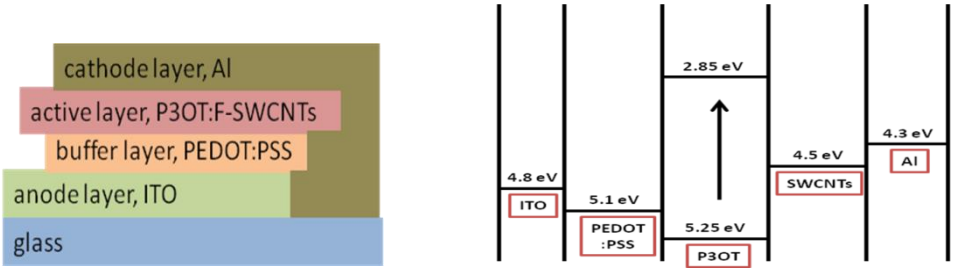

Fig. 1. Architecture of fabricated photovoltaic cells and band offset diagram of constitutive materials

2.3. Characterization techniques

Spectroscopic analyses of synthesized and functionalized SWCNTs were performed by Raman measurements using a visible light laser with 532 nm excitation wavelength and energy of 2.33 eV. The type of fabricated single wall carbon nanotubes was determined by Kataura plot [23] and the mass loss induced by temperature was quantified by thermogravimetric analyses (TGA), under air, heating from 50°C to 900°C with 5°C/minute rate for synthesized and functionalized SWCNTs. Morphological features of SWCNTs and F-SWCNTs were investigated by field emission scanning electron microscopy (FESEM). The electrical and photoelectrical behavior of functionalized single wall carbon nanotubes (F-SWCNTs) and regioregular polymer based photovoltaic cells were analyzed, at room temperature, and compare with the results obtained for regioregular polymer active layer samples. Short-circuit current, open circuit voltage and fill factor were calculated in AM 1.5 conditions for all fabricated PV cells.

3. Results and discussion

3.1. Spectroscopic analyses

Radial breathing mode (RBM) of Raman spectra together with disorder induced mode (D-band) and tangential mode (G-band) of single wall carbon nanotubes and functionalized ones are presented in figure 2. RBM frequency region is a special band of SWCNTs and is localized between 150 cm^{-1} and 300 cm^{-1}, and for our synthesized SWCNTs this was found in the 152 cm^{-1} – 228 cm^{-1} range. D band is related to scattering on sp^3 carbon atoms while G-band with in-plane oscillations of sp^2 hybridized carbon atoms from the architecture of nanotubes [24, 25].

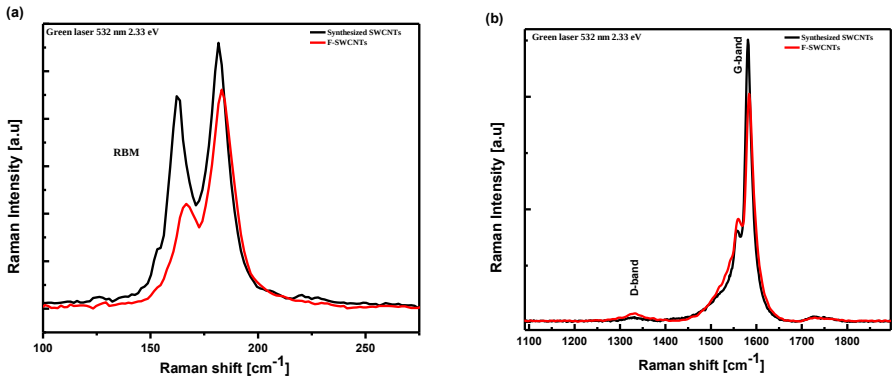

Fig 2. (a) Radial breathing mode of Raman spectra of synthesized SWCNTs (black curve) and F-SWCNTs (red curve); (b) D-band and G-band of synthesized SWCNTs (black curve) and F-SWCNTs (red curve). A 532 nm excitation wavelength was used for Raman measurements.

The Raman shifts of the RBM peaks were up and slightly smaller intensities were observed for F-SWCNTs indicating the appearance of localized defects on wall's structure due to nitric acid, favoring the attaching of different functional groups [26, 27]. Moreover, this behavior was confirmed by a small increase of D-band peak and by the decrease of G-band peak.

Using the equation describing the relationship between RBM vibrational frequency and diameter of the nanotubes, a distribution between 1.0 nm and 1.6 nm was found for our synthesized SWCNTs; these data are summarized in Table 1.

$d = \frac{c1}{(\omega - c2)}$, where d is the nanotubes' diameter, ω is vibrational frequency in the direction of radial breathing of the nanotubes, and $c1$ and $c2$ are constants with the following values: $c1 = 215\ cm^{-1}$, $c2 = 18\ cm^{-1}$. Kataura plot is presented in figure 3 and was used to

determine the type of our synthesized SWCNTs and showed a mixture between metallic and semiconductor type in about 50:50 percent ratio (see table 1).

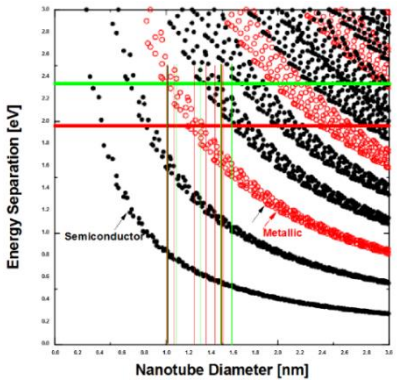

Fig. 3. Kataura plot of synthesized single wall carbon nanotubes.
The red points indicate metallic type and the black ones, semiconductor type.
Diameters' distribution of our fabricated SWCNTs is marked by vertical lines.

Table 1. Calculated diameters of synthesized SWCNTs and determination of their type

Raman shift [cm^{-1}]	SWCNTs diameter [nm]	SWCNTs type
152.70	1.6	Semiconductor
162.86	1.5	Semiconductor
181.90	1.3	Semiconductor
205.52	1.2	Metallic
220.48	1.1	Metallic
227.95	1.0	Metallic

3.2. Thermogravimetric measurements

TGA curves confirmed that mass loss induced by temperature was 70.78% for synthesized SWCNTs and 81.54% for the functionalized ones indicating that ratio between amorphous carbon and residual metallic catalysts decreased after functionalization (see figure 4). The TGA derivatives curves showed a decrease of onset temperature of F-SWCNTs most likely due to the presence of localized defects in walls' architecture, induced by nitric acid. TGA measurements and its derivatives confirmed that SWCNTs were successfully functionalized.

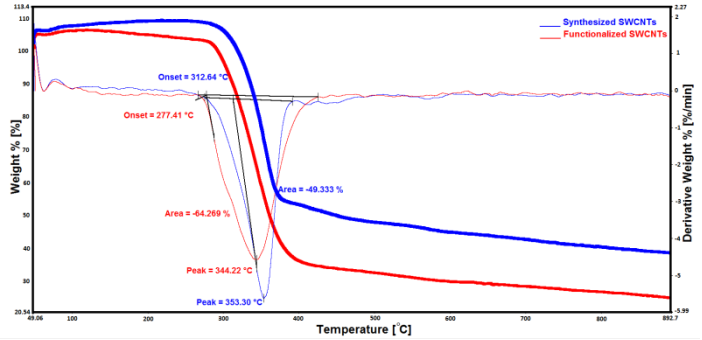

Fig. 4. TGA curves and its derivatives of SWCNTs and F-SWCNTs, recorded in air

3.3. Morphological investigations

Field emission scanning electron microscopy (FESEM) images of SWCNTs and F-SWCNTs are presented in figure 5, for different magnification orders.

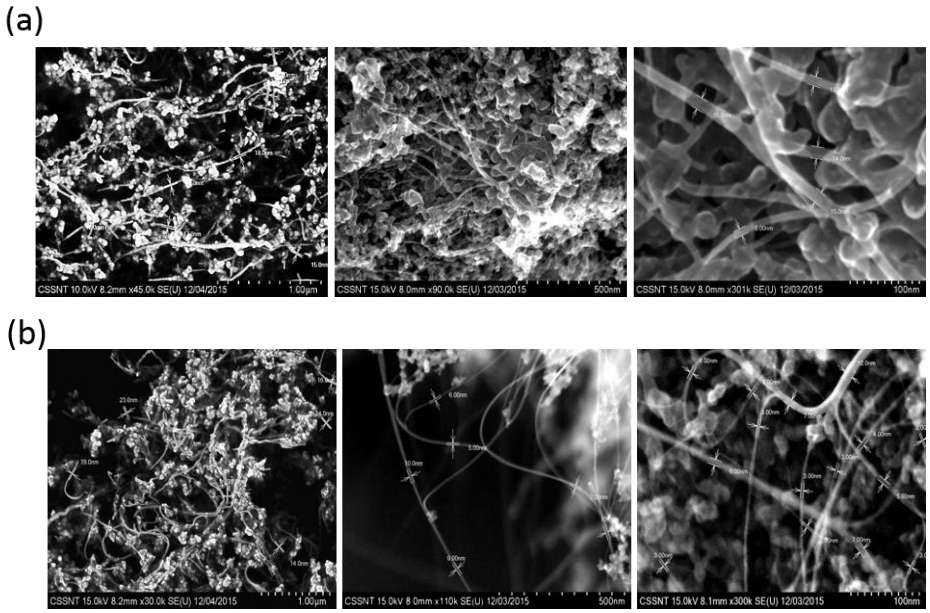

Fig. 5. (a) FESEM images of synthesized SWCNTs; (b) FESEM images of functionalized SWCNTs, for different magnification orders. A Hitachi SU8020 UHR Cold-Emission FE-SEM machine was used.

We observed bundles of SWCNTs surrounded by amorphous carbons and metal catalysts, while after functionalization the quantity of residual particles significantly decreased. Moreover, the dimension of bundles was reduced as a consequence of the success functionalization process. These results confirmed the thermogravimetric measurements.

3.4. Electrical and photoelectrical measurements of PV cells

External quantum efficiency spectra in 350 – 900 nm range of fabricated photovoltaic cells are presented in figure 6.

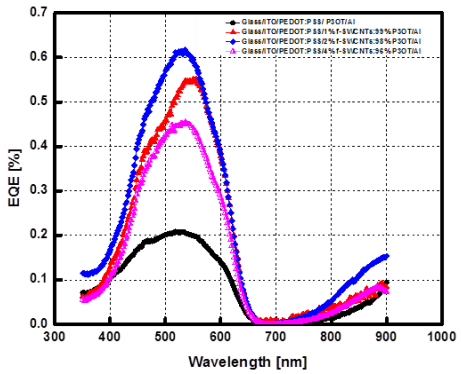

Fig. 6. Action spectra of glass/ITO/PEDOT:PSS/P3OT/Al (black curve), glass/ITO/PEDOT:PSS/F-SWCNTs(1%):P3OT/Al (red curve), glass/ITO/PEDOT:PSS/F-SWCNTs(2%):P3OT/Al (blue curve) and glass/ITO/PEDOT:PSS/F-SWCNTs(4%):P3OT/Al (pink curve) fabricated photovoltaic cells

Even external quantum efficiency small values (EQE is defined as the ratio between charge carriers collected to electrodes and the number of incident photons) were calculated for our fabricated photovoltaic cells, a significant improvement can be notice in the case of F-SWCNTs:polymer active layer samples. Our measurements proved an important increase of EQE values for glass/ITO/PEDOT:PSS/F-SWCNTs(2%):P3OT/Al PV cells compared with regioregular

polymer based devices. A bigger percent of functionalized single wall carbon nanotubes (4%) introduced more point-like defects in the structure of our hybrid samples affecting the photovoltaic performances by stopping or strangling charge carriers' transport.

For a complete photoelectrical characterization, current-voltage curves were drawn in AM 1.5 conditions and specific parameters were calculated for all fabricated PV cells.

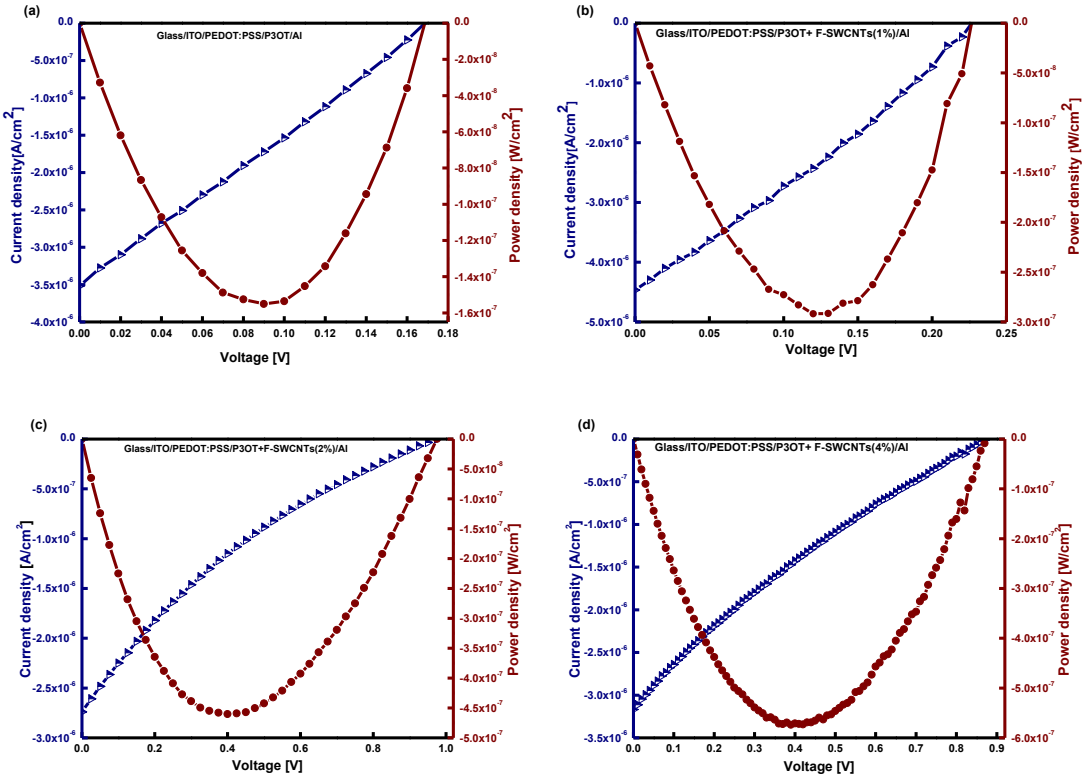

Fig7. I-V curves in AM 1.5 conditions of (a) glass/ITO/PEDOT:PSS/P3OT/Al, (b) glass/ITO/PEDOT:PSS/F-SWCNTs(1%):P3OT/Al, (c) glass/ITO/PEDOT:PSS/F-SWCNTs(2%):P3OT/Al and (d) glass/ITO/PEDOT:PSS/F-SWCNTs(4%):P3OT/Al photovoltaic cells

Specific parameters of our fabricated samples were calculated taking into account an active area of 0.4 cm^2 (see table 2).

Table 2. Calculated specific parameters of fabricated photovoltaic cells

Sample	J_{SC} (mA/cm^2)	V_{OC} (V)	Fill Factor (%)
glass/ITO/PEDOT:PSS/P3OT/Al	3.5×10^{-3}	0.17	26
glass/ITO/PEDOT:PSS/F-SWCNTs(1%):P3OT/Al	4.5×10^{-3}	0.23	28
glass/ITO/PEDOT:PSS/F-SWCNTs(2%):P3OT/Al	2.7×10^{-3}	0.98	17
glass/ITO/PEDOT:PSS/F-SWCNTs(4%):P3OT/Al	3.1×10^{-3}	0.88	21

All samples having a composite F-SWCNTs: regioregular polymer active layer have higher open circuit voltage compared with glass/ITO/PEDOT:PSS/P3OT/Al photovoltaic cells most likely due to the increasing of electrical conductivity by SWCNTs contribution. With a well-defined crystalline structure, SWCNTs offer easy charge carriers' transportation ways. Even if the calculated fill factor value is small, open-circuit voltage of glass/ITO/PEDOT:PSS/F-

SWCNTs(2%):P3OT/Al samples confirmed the external quantum efficiency obtained results. One may say a key factor to increase the photovoltaic performances of CNTs based structures is to control their arrangement [28]. Further studies are necessary to determine the appropriate conditions to increase the energy conversion efficiency.

4. Conclusions

SWCNTs with diameters between 1.0 nm and 1.6 nm were successfully synthesized and functionalized by nitric acid. Different percentages of F-SWCNTs, 1%, 2% and 4%, were mixed with P3OT, to prepare the photo-active layer of fabricated photovoltaic cells. An optimal percentage of 2% was determined for our prepared structures. The addition of F-SWCNTs increased the open-circuit voltage due to their well-defined crystalline structure that offers supplementary charge carriers' transportation ways compared with P3OT based photovoltaic cells, even though this polymer showed an early crystallization process, as thin film. The external quantum efficiency values were bigger for all samples having F-SWCNTs:P3OT active layer proving the that these blends with high homogeneity could be used successfully to the preparation of bulk-heterojunction photovoltaic cells with improved efficiency and stability.

Acknowledgements

This work was supported by Romanian Ministry of Education and Scientific Research and by Executive Agency for Higher Education, Research, Development and Innovation Funding, under Projects PCCA 2-nr. 166/2012 and ENIAC 04/2014. J. Al-zanganawee acknowledges also the support of the Ministry of Higher Education and Scientific Research of Iraq.

References

[1] G. Xiao, Y. Tao, J. Lu, Z. Zhang, Thin Solid Films **518**, 2822 (2010).
[2] S. Chaudhary, H. Lu, A.M. Müller, C.J. Bardeen, M. Ozkan, Nano Letters **7**, 1973 (2007).
[3] M. Girtan, Organic Electronics **14**, 200 (2013).
[4] L. Magherusan, P. Skraba, C. Besleaga, S. Iftimie, N. Dina, M. Bulgariu, C.G. Bostan, C. Tazlaoanu, A. Radu, L. Ion, M. Radu, A. Tanase, G. Bratina, S. Antohe, J. Optoelectron. Adv. Mater. **12**, 212 (2010)
[5] E. Lopez-Elvira, B. Garcia-Perez, J. Colchero, E. Palacios-Lidon, Synthetic Metals **161**, 1651 (2011)
[6] V. Causin, C. Marega, A. Marigo, L. Valentini, J.M. Kenny, Macromolecules **38**, 409 (2005)
[7] M.C. Arenas, N. Mendoza, H. Cortina, M.E. Nicho, H. Hu, Solar Energy Materials and Solar Cells **94**, 29 (2010)
[8] E. Itoh, Y. Takamizawa, K. Miyairi, Japanese Journal of Applied Physics **47**, 509 (2008)
[9] T. Ishwara, D.D.C. Bradley, J. Nelson, P. Ravirajan, I. Vanseveren, T. Cleij, D. Vanderzande, L. Lutsen, S. Tierney, M. Heeney, I. McCulloch, Applied Physics Letters **89**, 252102 (2006)
[10] T.J. Prosa, M.J. Winokur, J. Moulton, P. Smith, A. Heeger, Macromolecules **25**, 4364 (1992)
[11] T. Erb, S. Raleva, U. Zhokhavets, G. Gobsch, B. Stuhn, M. Spode, O. Ambacher, Thin Solid Films **450**, 97 (2004)
[12] S. Hugger, R. Thomann, T. Heinzel, T. Thurn-Albrecht, Colloid and Polymer Science **282**, 932 (2004)
[13] S. Joshi, S. Grigorian, U. Pietsch, P. Pingel, A. Zen, D. Neher, U. Scherf, Macromolecules **41**, 6800 (2008)
[14] B. Perez-Garcia, J. Abad, A. Urbina, J. Colchero, E. Palacios-Lidon, Nanotechnology **19**, 065709 (2008)
[15] J. Abad, B. Perez-Garcia, A. Urbina, J. Colchero, E. Palacios-Lidon, European Polymer Journal **44**, 2506 (2008)

[16] K. Guru, S.B. Mishra, K.K. Shukla, Applied Surface Science **349**, 59 (2015)
[17] L. Liu, A.H. Barber, S. Nuriel, H.D. Wagner, Advanced Functional Materials **15**, 975 (2005)
[18] R. Bandyopadhyaya, E. Nativ-Roth, O. Regev, R. Yerushalmi-Rozen, Nano Letters **2**, 25 (2002)
[19] R. Shvartzman-Cohen, Y. Levi-Kalisman, E. Nativ-Roth, R. Yerushalmi-Rozen, Langmuir **20**, 6085 (2004)
[20] C. Velasco-Santos, A.L. Martinez-Hernandez, M. Lozada-Cassou, A. Alvarez-Castillo, V.M. Castano, Nanotechnology **13**, 495 (2002)
[21] M.E. Rincon, G. Alvarado-Tenorio, M.G. Vargas, E. Ramos, M. Sanchez-Tizapa, Thin Solid Films **597**, 70 (2015)
[22] F.H. Gojny, J. Nastalczyk, Z. Roslaniec, K. Schulte, Chemical Physics Letters **370**, 820 (2003)
[23] M. Kusaba, Y. Tsunawaki, Thin Solid Films **506-507**, 255 (2006)
[24] M.S. Dresselhaus, P.C. Eklund, Advances in Physics **49**, 705 (2000)
[25] P.C. Eklund, J.M. Holden, R.A. Jishi, Carbon **33**, 959 (1995)
[26] R. Graupner, Journal of Raman Spectroscopy **38**, 673 (2007)
[27] S. Hussain, P. Jha, A. Chouksey, R. Raman, S.S. Islam, T. Islam, P.K. Choudhary, Journal of Modern Physics **2**, 538 (2011)
[28] L. Baschir, S. Antohe, A. Radu, R. Constantineanu, S. Iftimie, M. Popescu, I.D. Simandan, Digest Journal of Nanomaterials and Biostructures **8**, 1645 (2013)